CHAPTER 5

ANISOTROPY OF MAGNETIC SUSCEPTIBILITY STUDIES

5.1. INTRODUCTION

This chapter presents results from *Anisotropy of Magnetic Susceptibility* (AMS) study on rocks of the Lunavada region and the tectonic interpretations using the AMS data. The author finds it essential to briefly describe the theory on which AMS study is based prior to presenting his own data.

When magnetic field is applied to any substance the electron spins precess and a magnetization is produced in a direction parallel or opposite to that of the applied field. This is referred to as induced magnetization and the strength of induced *magnetization (M)* can be directly related to the strength of *applied field (H)*. The constant of proportionality is the susceptibility (K). The *magnetization, M*, is given by the formula

$$M=KH=KB/\mu_0$$

where M is the magnetic dipole moment per unit volume (in A/m), H is the magnetic field strength (A/m), B is the magnetic field measured in Tesla and μ_0 is the permeability of free space ($4\pi \times 10^{-7}$ henry/m) (Tarling and Hrouda, 1993).
The above equation can be rewritten for magnetic susceptibility as

$$K=M/H$$

It is clear that susceptibility is a dimensionless quantity and is represented as SI units. However, it is dependent on the temperature and strength of the applied field and is therefore not a constant for any given material. As far as tectonic applications of magnetic susceptibility on rocks are concerned, the measurements are usually made in the weak/low field ($\leq$ 1mT).

Certain materials have the same strength of induced magnetization (and hence the susceptibility) in every direction to which a external weak field is applied. Such materials are considered as ***magnetically isotropic***. On the other hand, there are certain materials which have a different strength of induced magnetization in different directions to which the weak external magnetic field of constant strength is applied. Such substances are termed as ***magnetically anisotropic*** and these have a anisotropic magnetic susceptibility which is referred to as the ***Anisotropy of Magnetic Susceptibility*** or ***(AMS)***. The variation of the susceptibility in different directions can be visualized as an ellipsoid generally referred to as the *susceptibility ellipsoid* (Tarling and Hrouda, 1993). It has three principal axes - long, intermediate and short. The greatest intensity of magnetization is induced along the long axis and the weakest intensity is induced along the short axis. The principal susceptibilities (in SI units) are represented as K_1, K_2 and K_3 where $K_1 \geq K_2 \geq K_3$ and these have been interpreted to correspond to sedimentary, magmatic or tectonic fabrics (Graham, 1954; Singh et. al. 1975, Hrouda, 1982; Kligfield et al, 1977, 1982; Owens and Bamford, 1976; Owens and Rutter, 1978; Goldstein, 1980). It has been shown that a good correspondence exists between the orientations of principal axes of the susceptibility ellipsoid and orientations of the principal axes of the strain ellipsoid in tectonically deformed rocks (Hrouda and Janák, 1976; Rathore, 1979, Borradaile and Tarling, 1981, 1984; Hrouda, 1982; Borradaile and

Mothersill, 1984; Borradaile, 1987; 1991; Borradaile and Alford, 1987; Borradaile and Henry, 1997).

5.2. AIMS OF AMS STUDY ON THE LUNAVADA PRE-CAMBRIAN ROCKS

The aims of carrying out AMS study on the rocks of the Lunavada region were two fold.

(a) Strain analysis: Exposures of good mesoscopic folds are scarce in the study area. Therefore, in such an area the AMS was thought to be a good technique to understand the type of strain.

(b) Analysis of the deformation episodes: Magnetic studies on tectonized rocks have in many areas of the globe yielded magnetic fabric which sometimes does not show any parallelism with the mesoscopic fabric and these have been interpreted to indicate later superimposed fabrics on the mesoscopically recognizable structures (Stacey et. al., 1960; Goldstein, 1980). It has been shown in Chapter 4 that D_3 deformation was weak and gave rise to open folds on limbs of regional scale F_1-F_2 folds, a fact which was worked out with a rigorous structural analysis. This third folding has not left significant mesoscopic imprint on the rocks. In such a situation, the AMS data was used as a tool to investigate the effect of this late deformation on rocks. This has enabled a better evaluation of the tectonics of the Lunavada region.

5.3. AMS DATA

Oriented samples from 12 different locations around Lunavada and Santrampur were collected to have a spatial distribution/representation from the whole region. A total of 40 cylindrical cores (26 mm x 22 mm) from these samples were analyzed for the AMS study. The samples comprised schists, quartzites and calc-silicates. The AMS measurements were made with the KLY-2 Kappabridge (Geofyzika Brno, Czech Republic) in the low field and the data were analyzed using the special software available with the Kappabridge. The measurements gave magnitude and orientations of the three principal axes of the susceptibility ellipsoid viz. K_1, K_2 and K_3 where $K_1 \geq K_2 \geq K_3$, the mean susceptibility (K_m), degree of anisotropy (P_j), shape parameter (T), magnitude of foliation (F) and lineation (L). Table 5.1 gives AMS data. The mean susceptibility of schists and calc-silicates was found to be more than 240 x 10^{-6} SI units. Most of the quartzites were recorded to have a positive mean susceptibility of around 50 x 10^{-6} SI and above although a few have lower mean susceptibility. The higher mean susceptibilities in schists and calc-silicates are on account of higher proportion of paramagnetic minerals like micas and chlorite (phyllosilicates) and their relative scarcity in quartzites. Quartz is a diamagnetic mineral and has a mean susceptibility of -13.5 x 10^{-6} (Hrouda, 1986). Microscopic examination of the analysed quartzites showed that most of them contain some mica. This results in positive values of the mean susceptibility of the quartzites.

Table. 5.1

AMS data for rocks of the Lunavada region. (K_m=mean susceptibility; F=magnetic foliation; L=magnetic lineation; P_j=degree of anisotropy; T=shape parameter; K_{max}, K_{int} and K_{min} represent magnitudes of maximum, intermediate and minimum axis of the magnetic ellipsoid; D/I represent the direction and amount of dip of principle axes of magnetic ellipsoid (in degrees).

Sample No.	Core No.	K_m	F	L	P_j	T	K_{max}	K_{int}	K_{min}	K_{max}-D/I	K_{int}-D/I	K_{min}-D/I
CS	1	256.6	1.037	1.008	1.048	0.632	1.0174	1.0093	0.9733	313/27	055/22	178/53
CS	2	246.3	1.035	1.009	1.046	0.588	1.017	1.0083	0.9747	301/21	042/25	176/57
CS	3	266.2	1.051	1.007	1.064	0.759	1.021	1.0143	0.9647	316/30	055/14	167/56
CS	4	249.3	1.057	1.007	1.07	0.782	1.0227	1.016	0.9613	300/22	040/23	172/58
AS	1	329	1.085	1.007	1.103	0.832	1.0316	1.0242	0.9442	324/43	060/06	157/46
AS	2	285.9	1.072	1.007	1.089	0.818	1.0276	1.0207	0.9518	338/47	069/01	160/43
AS	3	315.1	1.082	1.008	1.101	0.8	1.0315	1.0229	0.9456	329/42	066/08	165/47
LS	1	375.1	1.065	1.032	1.1	0.31	1.0419	1.0096	0.9485	359/34	266/05	169/56
LC	1.1	255.6	1.009	1.002	.1.011	0.586	1.0043	1.0021	0.9936	246/46	043/42	143/11
LC	1.2	242.7	1.013	1.006	1.02	0.379	1.0084	1.0024	0.9892	223/30	043/70	313/00
LC	2	243	1.01	1.001	1.012	0.74	1.0042	1.0028	0.993	221/31	037/59	130/02
LC	2.2	264.7	1.02	1.002	1.025	0.813	1.008	1.006	0.986	220/35	031/54	127/04
LC	3	429.4	1.022	1.013	1.036	0.241	1.0159	1.0028	0.9813	037/01	132/73	306/17
MQ	1.1	51.88	1.096	1.019	1.126	0.642	1.0429	1.0234	0.9337	328/24	058/01	152/66
MQ	1.2	50.85	1.108	1.021	1.142	0.647	1.0478	1.0263	0.9259	329/23	239/00	149/67
MQ	2	55.41	1.112	1.016	1.142	0.721	1.0458	1.029	0.9252	323/30	232/02	139/60
MQ	3.1	51.04	1.103	1.022	1.135	0.624	1.0466	1.0245	0.929	330/19	240/00	149/71
MQ	3.2	57.27	1.095	1.017	1.123	0.675	1.0412	1.0239	0.9349	336/17	245/01	150/72
MQ	4	50	1.105	1.024	1.14	0.596	1.0487	1.0241	0.9272	337/25	244/06	141/64
AQ	1.1	50.16	1.084	1.02	1.112	0.597	1.0397	1.0197	0.9406	172/23	067/31	291/50
AQ	1.2	70.65	1.068	1.009	1.085	0.74	1.0279	1.0183	0.9538	182/18	080/32	297/52

Sample No.	Core No.	K_m	F	L	P_j	T	K_{max}	K_{int}	K_{min}	K_{max}-D/I	K_{int}-D/I	K_{min}-D/I
AQ	2.1	54.01	1.077	1.023	1.106	0.516	1.0397	1.0165	0.9439	166/20	063/31	283/52
AQ	2.2	33.87	1.082	1.028	1.116	0.46	1.0445	1.0161	0.9394	162/22	060/29	283/52
AQ	3	37.8	1.051	1.021	1.075	0.387	1.0306	1.0091	0.9603	168/17	063/40	277/45
AQ	4.1	69.35	1.064	1.008	1.079	0.761	1.0258	1.0175	0.9567	187/23	079/36	302/45
AQ	4.2	41.59	1.065	1.012	1.084	0.67	1.0289	1.0166	0.9546	188/20	077/45	295/38
BS	1.1	56.62	1.025	1.021	1.046	0.075	1.0219	1.0011	0.9769	041/14	291/56	140/31
BS	1.2	53.4	1 018	1.012	1.031	0.167	1.0141	1.0017	0.9842	045/15	291/57	144/29
BS	2.1	60.44	1.025	11.018	1.044	0.161	1.0203	1.0023	0.9774	042/14	258/73	134/10
BS	2.2	59.96	1.017	1.02	1.038	-0.093	1.019	0.9989	0.9821	039/11	278/69	133/17
LQ	1.1	4.31	1.041	1.033	1.075	0.083	1.0351	1.002	0.9629	237/28	139/15	024/57
LQ	1.2	6.61	1.042	1	1.049	0.983	1.0139	1.0135	0.9726	145/00	235/28	055/62
LQ	2	1.14	1.187	1.095	1.305	0.248	1.1183	1.0214	0.8604	142/02	233/37	049/53
LQ	3	3.47	1.058	1.012	1.076	0.632	1.027	1.0144	0.9586	176/33	280/19	035/50
SQ	1	-3.03	1.011	1.114	1.126	-0.829	-1.0772	-0.9666	-0.9562	219/57	068/30	330/13
SQ	2	-3.79	1.044	1.079	1.126	-0.307	-1.0659	-0.9877	-0.9463	214/68	062/19	329/09
RQ	1	-4.2	1.051	1.099	1.156	-0.342	-1.0811	-0.9834	-0.9355	149/61	262/12	357/26
RQ	2	-4.68	1.066	1.096	1.168	-0.215	-1.0836	-0.9888	-0.9276	155/65	264/09	358/23
GQ	2	2.22	1.062	1.103	1.174	-0.275	1.0871	0.9854	0.9276	003/27	262/19	142/56
GQ	3	7.21	1.055	1.006	1.068	0.792	1.0219	1.0157	0.9624	049/05	317/17	155/72
KQ	1	0.83	26.538	1.513	57.185	0.304	1.7797	1.1759	0.0443	136/36	035/16	285/50
KQ	1.1	0.99	5.465	1.393	8.826	0.351	1.6222	1.1647	0.2131	138/35	036/17	284/50
KQ	2	-2.22	1.076	1.289	1.387	-0.606	-1.2013	-0.9323	-0.8664	122/53	028/03	295/36
KQ	3	0.45	-	-	-	0.324	1.6185	0.9127	-0.4688	138/42	032/17	285/43

5.4. INTERPRETATION OF AMS DATA

Orientations of K_1, K_2 and K_3 axes have been plotted on *Equal Area Net* (Schmidt Net) (Fig. 5.1). The plane passing through K_1, and K_2 is referred to as the *magnetic foliation (F)* and this is plotted as a continuous great circle in Fig. 5.1. The planar structure (generally S_0) recorded mesoscopically at each sample locality has been plotted as dashed great circle in each lower hemisphere stereographic projection in Fig. 5.1. A close similarity is seen between magnetic data and field structural data for the localities from which the samples for AMS were studied. However, there is a significant deviation of magnetic foliation from the planar structural elements in some of quartzites (e.g. LQ, RQ and SQ, see Fig. 5.1). The LQ lies exactly on the nose of a D_3 fold. The magnetic foliation has a NW-SE orientation and this is parallel to the orientation of axial trace (S_3) of D_3 folds in the locality where the LQ sample lies (Fig. 5.1). Based on this similarity of AMS fabric with the regional macroscopic structure, the magnetic foliation is interpreted to be on account of D_3 deformation although locally there is no mesoscopic scale imprint of the late deformation. The author would like to highlight here that the structural analysis of field data from this part of study area (domain IX in section 4.3) also led to determination of F_3 fold axis.

Is it rotated strain due to D2

The samples RQ and LQ show NE-SW trending magnetic foliations which are similar to the trend of the axial plane (S_2) of D_2 folds recorded in other parts of the study area. The localities of the RQ and SQ samples do not show any mesoscopic D_2 folds and show development of N-S trending S_0/S_1 foliations related to the D_1 deformation. However, the presence of NE-SW trending

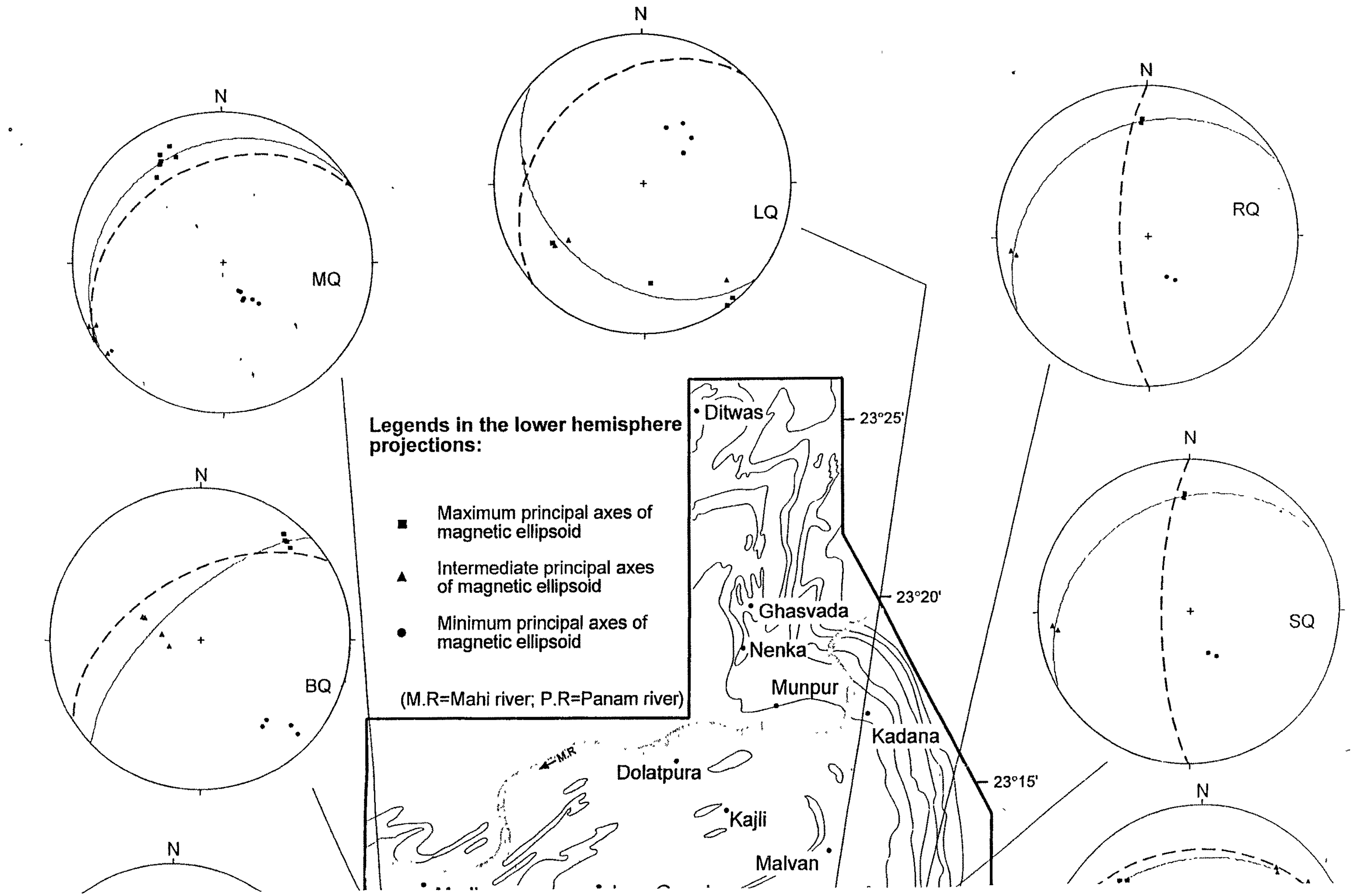
N
MQ
N
LQ
N
RQ
N
BQ
N
SQ
N
N
Legends in the lower hemisphere projections:
Maximum principal axes of magnetic ellipsoid
Intermediate principal axes of magnetic ellipsoid
Minimum principal axes of magnetic ellipsoid
(M.R=Mahi river; P.R=Panam river)
Ditwas
23°25'
23°20'
23°15'
Ghasvada
Nenka
Munpur
Kadana
M.R
Dolatpura
Kajli
Malvan

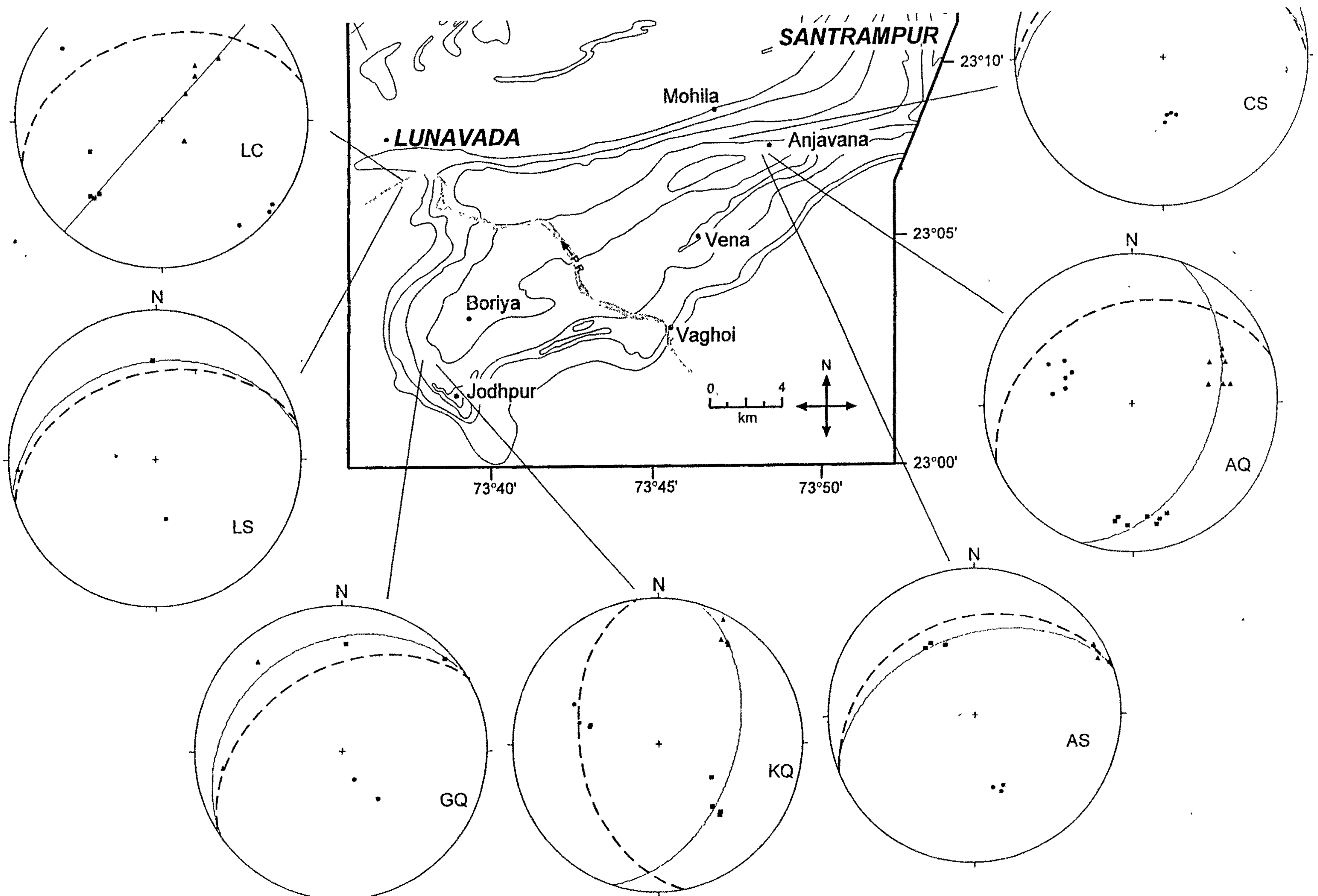

Fig. 5.1. AMS orientation data plotted as lower hemisphere projections for the area around Lunavada and Santrampur Complete great circles represent the magnetic foliation Dashed great circles represent the planar structure recorded in the field.

magnetic foliations in the SQ and RQ samples clearly points to local development of D_2 folds although they are not exposed mesoscopically. Moreover, SQ and RQ lie on the limb of a megascopic regional D_3 fold. The absence of NW-SE trending magnetic foliations in this area indicates that the D_3 deformation was not strong enough to modify the magnetic fabric on the limbs of the fold. On the other hand the sample LQ lies on the nose of D_3 fold and this is where the effect of D_3 was strong enough to affect the magnetic fabric in the rock, thus resulting in the development of NW-SE trending magnetic foliations.

Jelinek plots (P_j vs. T), Fig. 5.2 a, b, c show that most of the samples studied fall in the oblate field (flattening field) and a few cores from the quartzites fall in the prolate field (constrictional field). For tectonic interpretations, the susceptibility ellipsoid is considered to correspond to the strain ellipsoid (Hrouda and Janák, 1976; Rathore, 1979; Borradaile and Tarling, 1981, 1984; Hrouda, 1982; Borradaile and Mothersill, 1984; Borradaile, 1987; 1991; Borradaile and Alford, 1987; Borradaile and Henry, 1997). Therefore, AMS data can also be represented by the *Flinn diagram* which is usually used to analyze the type of strain in structural geology. For AMS data, the Flinn type diagram is prepared by plotting the foliation, F (K_2/K_3) as X axis against the lineation, L (K_1/K_2) as Y axis. The Flinn type (Fig. 5.3) plot was prepared for the different samples and a good correlation was found between the Flinn and the Jelinek plots (Fig.5.2). The Flinn type plot for the Bhadaria quartzite (Fig. 5.4) is most interesting and requires discussion. It is seen from this figure that the cores from the Bhadaria quartzite fall very close to the k=1 line which separates the prolate and the

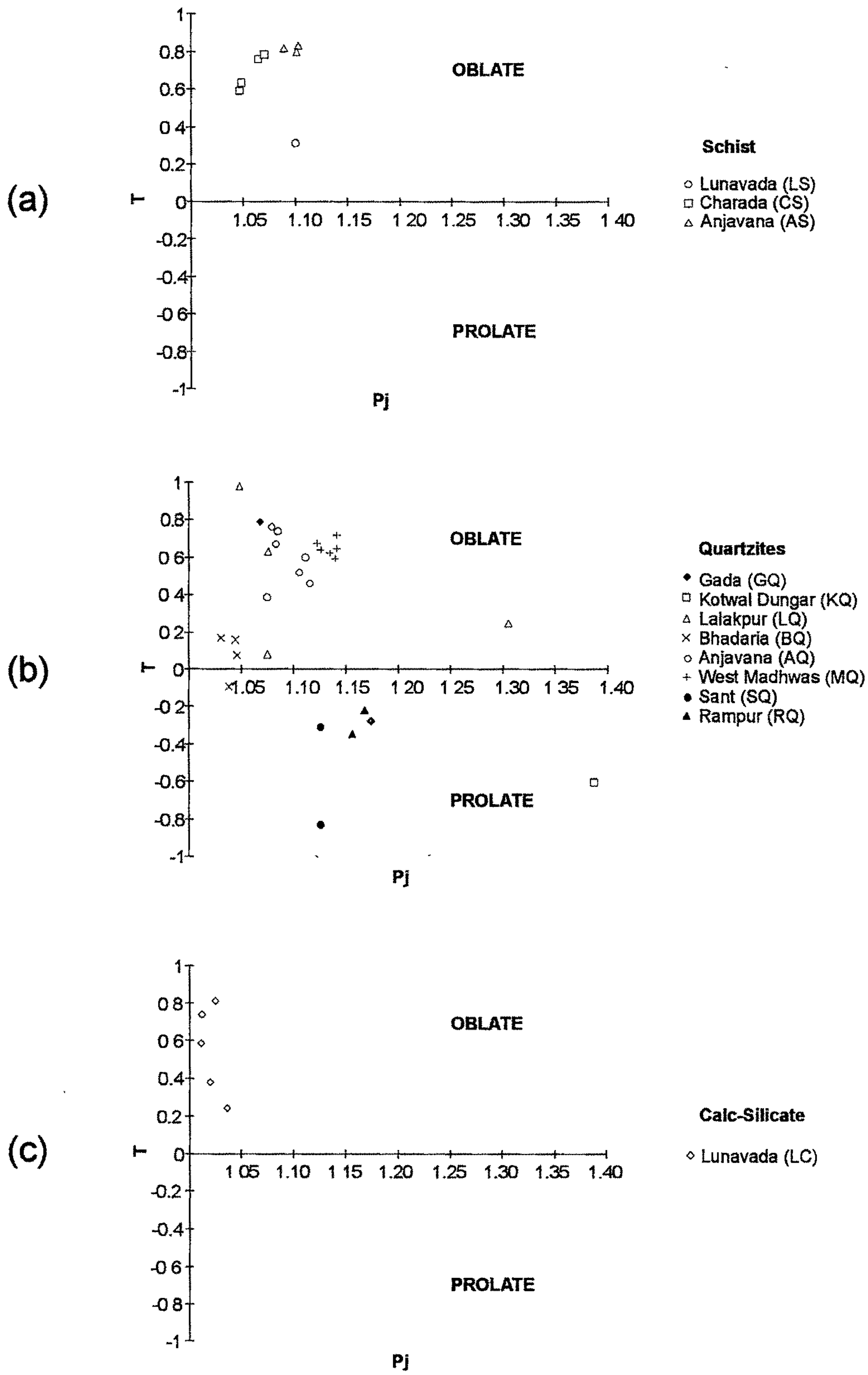

Fig.5.2. Jelinek Plots for Schists (a), Quartzites (b) and Calc Silicates (c) occurring in the study area around Lunavada and Santrampur.

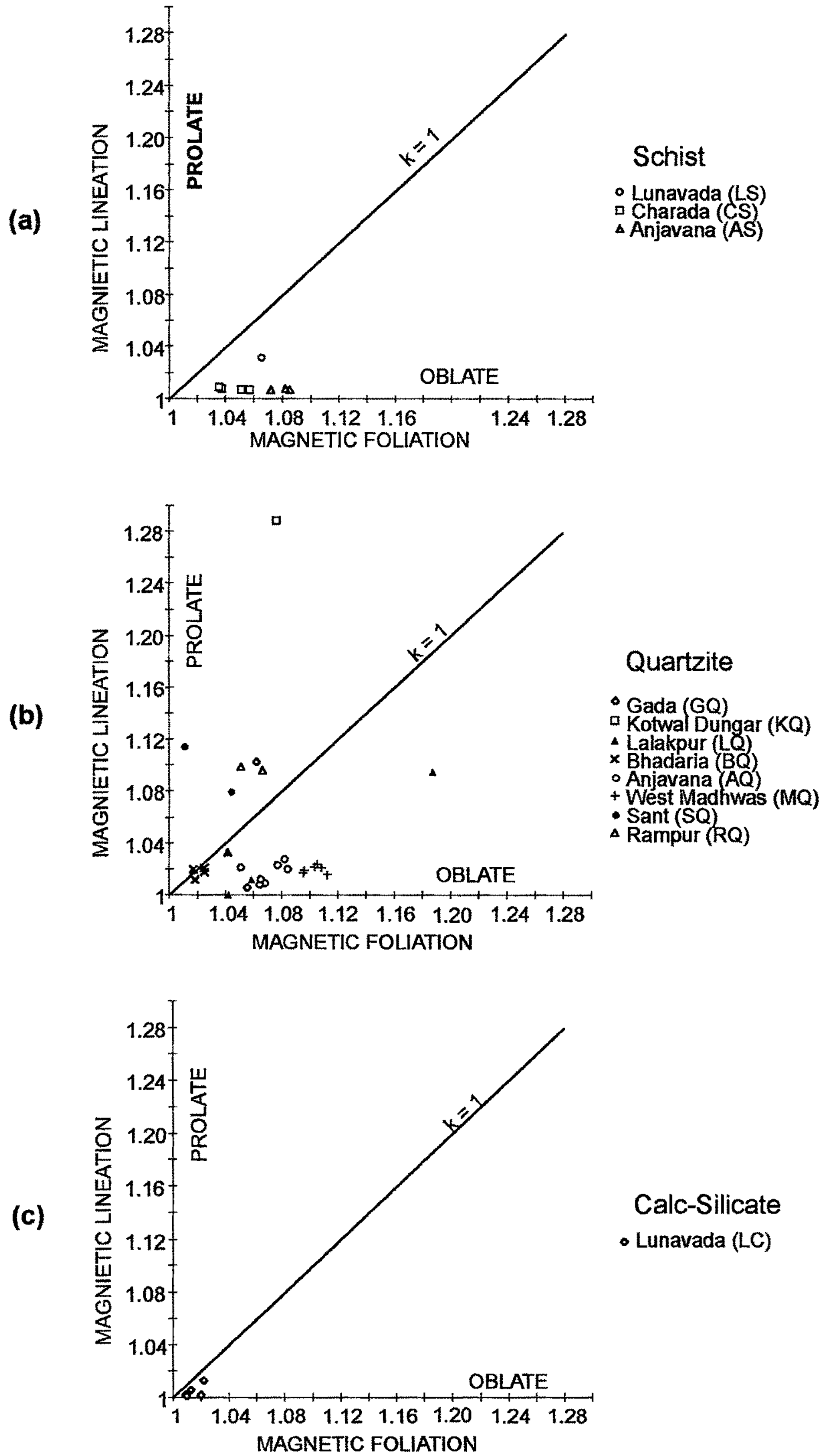

Fig.5.3. Flinn type plots prepared from AMS data for (a) schists, (b) quartzites and (c) calc-silicates occurring around Lunavada and Santrampur.

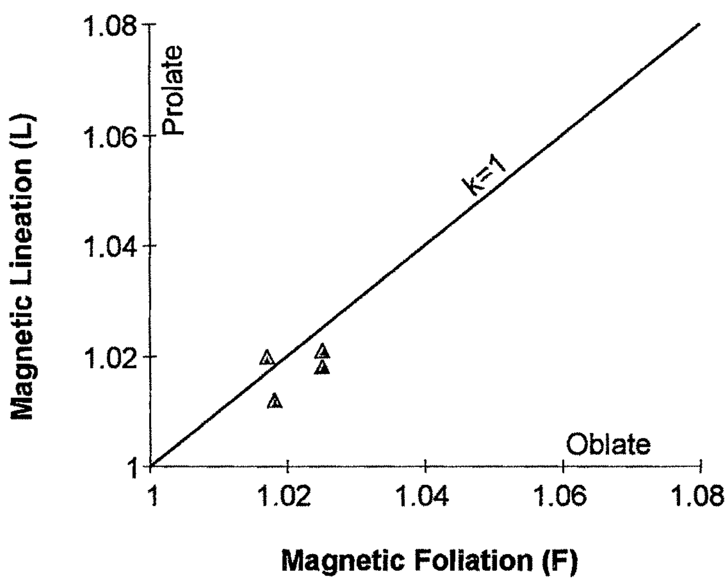

Fig.5.4. Flinn diagram for the quartzites from Bhadaria (BQ).

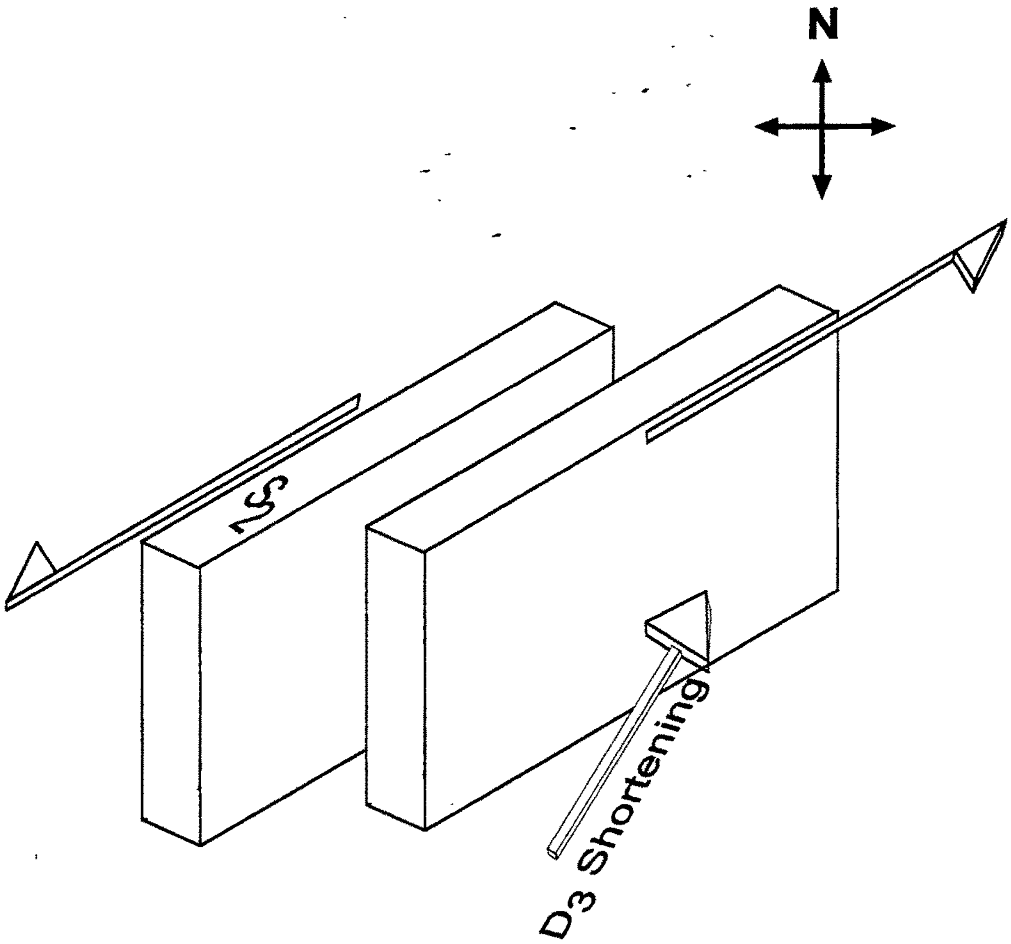

Fig.5.5. Sketch showing the orientation of S2 foliations at an oblique angle to the D3 shortening which could enable sinistral shearing parallel to S2.

oblate fields. This could be either an indication of plane strain or of simple shear or a component of simple shear in the regional strain of this area.

5.5. DISCUSSION

The above study has shown that the AMS study has been an important complement to the routine tectonic study techniques. It has been shown that a good correlation exists between the AMS data and the field structural data in the Lunavada region. The AMS data generally corresponds to the bedding plane or the foliation planes. Magnetic studies on tectonized rocks in some other parts have yielded magnetic fabric which sometimes does not show any parallelism with the mesoscopic fabric, but then these could be interpreted to indicate later superimposed fabrics on the mesoscopically recognizable structures (Stacey et al., 1960; Goldstein, 1980). In the present study area also there are a few localities where there is lack of correspondence between the field and magnetic data which is interpreted to be due to the effect of F_2 folding in RQ and SQ samples; in the LQ sample it is interpreted to be on account of F_3 folding. It is important to mention that in the above samples, the AMS fabric reveals orientations of structures which are not recordable in the field on the mesoscopic scale. This not only authenticates the conclusions but also establishes the relevance of the use of AMS studies in structural geology.

Besides the above, a correlation between the microscopic fabric and the AMS data of the schists warrants discussion. A microstructural study of the Anjavana schist (AS), Charada schist (CS) and Lunavada Schist (LS) samples has shown that there is a increase in the intensity of deformation in that order. The AS sample shows presence of a axial plane cleavage but is devoid of any crenulation cleavage. The foliation is defined by parallel alignment of micas. Thin sections of the CS sample show the presence of a stronger foliation compared to the AS sample while the LS schists have a strongly developed crenulation cleavage which has got homogenized to stage 6 of crenulation cleavage development of Bell and Rubenach (1983) and Mamtani and Karanth (1996 a ; pl. see chapter 5 for details on origin of crenulation cleavage). Thus, the fabric preserved within the three schists from AS through CS to LS indicates an increasing fabric gradient in that order. The Jelinek plot of these three schist samples (Fig. 5.2a) show a gradual progression towards the plane strain (i.e. progression towards T = 0) from sample AS to LS which is in good correspondence with the intensity of deformation observed microstructurally. This ideally establishes the authenticity of the applicability of AMS studies in strain analysis.

The plots for cores from Bhadaria quartzites which fall close to the k=1 line in Fig. 5.4 are an indication of a simple shear component in the deformational history of the Lunavada Group of rocks. This simple shear component, in likelihood is a reflection of the highly tectonized NE-SW trending shear zone to the N of Lunavada shown on the tectonic map of the AMB (Fig. 3.1c). Moreover, field studies have shown that the axial planes of the F_1-F_2 folds also trend NE-SW. The NW-SE to WNW-ESE trend of the F_3 axial traces indicates that the D_3 deformation occurred due to NE-SW or NNE-SSW shortening. The NE-SW trending axial plane structures (cleavages, foliations and fractures) that developed during the F_1-F_2 foldings in the area are therefore at a favourable angle to the shortening direction of D_3 deformation. Consequently sinistral shearing (Fig. 5.5) is possible parallel with these structures. This process is interpreted here as the main cause of the sinistral shear zone to the north of Lunavada and Kadana and the proximity of the cores from the Bhadaria sample to the k=1 line in Fig. 5.4 is a manifestation of this shearing.